

Shadow of Bonanno–Reuter Black Hole in Plasma Medium: Insights from EHT Sgr A* Observations

Shubham Kala ^{1,*}

¹*The Institute of Mathematical Sciences, C.I.T Campus, Taramani-600113, Chennai, Tamil Nadu, India*

We investigate the properties of black hole shadows in the renormalization group (RG) improved Bonanno–Reuter spacetime, incorporating quantum gravitational corrections via the scale-dependent parameter ($\tilde{\omega}$) in a plasma medium. Light propagation in a non-uniform, pressureless plasma with a radial density profile is analyzed through modified equations of motion. The black hole shadow angular radius is computed, and its dependence on $\tilde{\omega}$ and the plasma index is analyzed. The analysis of specific limiting cases indicates systematic deviations of the black hole shadow relative to the classical Schwarzschild limit. Using Event Horizon Telescope (EHT) observations of Sgr A*, we place constraints on $\tilde{\omega}$. Furthermore, within the considered parameter range, plasma and quantum-gravity effects exhibit an observational degeneracy, which future high-resolution measurements with the next-generation EHT are expected to break, thereby providing tighter constraints on the model parameters.

Keywords: General Relativity, Renormalization Group Improved Black Hole, Black Hole Shadow, Plasma Medium, EHT Collaboration

I. INTRODUCTION

Black holes (BHs), which are solutions of general relativity (GR), are among the most fascinating objects in the universe [1, 2]. The study of BH shadow has become a crucial method for exploring the strong gravitational field near compact objects, offering insights into spacetime geometry and fundamental physics. When light from an accretion disk or background source approaches a BH, gravitational lensing causes it to bend around the compact object [3–6], creating a dark region on the observer’s sky known as the shadow [7, 8]. The BH shadow represents the projected silhouette of the photon region as seen by a distant observer, shaped by the underlying spacetime curvature near the event horizon [9]. Theoretical work by Synge [10] and Bardeen [11] laid the foundation for understanding shadow formation in Schwarzschild and Kerr geometries. The influence of charge and spin on the BH shadows was explored by Takahashi [12], demonstrating notable deviations from the standard Schwarzschild BH (SBH) shadow. More recent studies by Falcke et al. [13], Johannsen et al. [14], and Konoplya et al. [15, 16] have extended the theoretical framework of BH shadows to include realistic astrophysical environments and to test deviations from GR in alternative theories of gravity.

The breakthrough observational confirmation came with the EHT collaboration, which imaged the shadow of the supermassive BH M87* (Akiyama et al., 2019), providing the first direct evidence of horizon-scale structure [17]. This achievement has sparked widespread interest in shadow-based tests of gravity, with numerous theoretical studies examining how modifications to GR, such as those arising from scalar-tensor theories, nonlin-

ear electrodynamics, or extra-dimensional models, affect the size and shape of BH shadows [18, 19]. In particular, the shadow’s sensitivity to spacetime geometry makes it a valuable probe for constraining BH parameters and for distinguishing between different gravitational theories in future high-resolution observations.

In realistic astrophysical environments, BHs are rarely isolated; they are often surrounded by hot, ionized matter in the form of plasma. This plasma may arise from accretion flows, stellar winds, or interstellar media, and its distribution can significantly affect the propagation of light in the vicinity of the BH [20]. Since plasma introduces a frequency-dependent refractive index, it modifies null geodesics and breaks the equivalence between geometrical and optical paths [21]. Several studies, including those by Perlick et al. [22–24] and Rogers [25], have extended the theory of gravitational lensing to include dispersive effects of plasma, showing that the presence of plasma alters the apparent position and brightness of lensed images, as well as the shape of the BH shadow [26–32].

Building on this, various authors have investigated the influence of plasma environments, both homogeneous and inhomogeneous, on BH shadows in the vicinity of different BH solutions arising from GR as well as alternative theories of gravity. Studies by Bisnovatyi-Kogan et al. [33], Attamurotov et al. [29, 34–36], Övgün et al. [37–39] and Perlick Tsupko [22], Chowdhuri et al. [40] and Kala et al. [41–43] have shown that such plasma profiles can either enlarge or shrink the BH shadow depending on the photon frequency and plasma parameters. These findings underscore the importance of incorporating plasma effects when modeling the optical appearance of BHs, especially in the context of interpreting high-resolution observations from instruments like the EHT.

RG improved BH solutions incorporate quantum gravity (QG) corrections by allowing gravitational couplings to run with scale [44]. In asymptotically safe grav-

*Electronic address: shubhamkala871@gmail.com

ity (ASG), these corrections modify classical metrics at high energies while recovering GR in the infrared [45, 46]. Quantum-corrected Kerr geometries were studied by Reuter and Tuiran [47], and thermodynamic implications by Becker and Reuter [48]. RG improvements in scenarios with large extra dimensions were explored by Burschil and Koch [49]. Recent works focus on observational signatures: shadows under accretion [50], rotating cases [51], plasma environments [52], and quasinormal modes [53], highlighting the phenomenological significance of RG improved models. Investigating the shadow of RG improved BHs in the presence of an astrophysical plasma medium is important for understanding how QG effects manifest in realistic observational settings. Plasma influences the propagation of light, and combined with deviations from GR, may lead to distinctive shadow features detectable by current or future telescopes.

The paper is organized as follows: In Section II, we introduce the RG group improved BH and its geometry. In Section III, we formulate the governing equations for the propagation of the light in plasma medium. Section IV focuses on the BH shadow and the constraints on its parameters based on EHT observations of Sgr A*. Finally, we present our conclusions in Section V.

II. BONANNO–REUTER BLACK HOLE

The Bonanno–Reuter BH (BRBH) emerges from the RG improvement of the classical Schwarzschild solution within the framework of ASG. In this approach, quantum gravitational effects are incorporated through a scale-dependent Newton’s constant $G(k)$, where k is an energy scale identified with the inverse of the radial coordinate r . The effective Newton’s constant is modeled as [44]

$$G(r) = \frac{G_0 r^3}{r^3 + \tilde{\omega} G_0 (r + \gamma G_0 M)}, \quad (1)$$

where G_0 denotes the infrared (low-energy) Newton’s constant. The running coupling $G(r)$, given in Eq. (1), when substituted into the Schwarzschild lapse function $f(r) = 1 - 2G(r)M/r$, leads to the RG-improved metric:

$$ds^2 = -f(r) dt^2 + \frac{dr^2}{f(r)} + r^2 d\Omega^2, \quad (2)$$

with the lapse function explicitly given by [54],

$$f(r) = 1 - \frac{2G_0 M r^2}{r^3 + \tilde{\omega} G_0 (r + \gamma G_0 M)}. \quad (3)$$

Here, the parameter $\tilde{\omega}$ is treated as a free parameter and represents the first non-trivial QG correction appearing in the large-distance expansion of the RG improved coupling. The constant γ is an interpolation parameter associated with the specific choice of cutoff identification in the RG improvement scheme. As noted in the original work [44], setting $\gamma = 0$ leads to essentially the

same qualitative properties of the improved BH spacetime. Therefore, in the present work, we fix γ to a positive constant and do not vary it in the shadow analysis, since it does not qualitatively affect the shadow characteristics. This quantum-corrected BH geometry asymptotically approaches the Schwarzschild solution at large radial distances, with subleading quantum corrections of order $\mathcal{O}(1/r^3)$. In the near-core region, the spacetime smoothly transitions to an effective de-Sitter geometry, characterized by an effective cosmological constant $\Lambda_{\text{eff}} \sim 1/r_0^2$, thereby resolving the central curvature singularity. Depending on the values of the BH mass M and the QG parameter $\tilde{\omega}$, the spacetime can exhibit two horizons (inner and outer), a single degenerate (extremal) horizon, or no horizon at all. For masses below a critical value M_{cr} , no event horizon forms, leading to a horizonless, soliton-like remnant. Such features are well-known consequences of QG corrections and may give rise to potential observational signatures, including modifications of BH shadows and possible gravitational-wave echoes. In Fig. 1, we plot the metric function $f(r)$ as a function of the radial coordinate r for representative values of the mass parameter M and the QG correction parameter $\tilde{\omega}$. The figure illustrates how variations in $\tilde{\omega}$ modify the causal structure of the BRBH spacetime. Specifically, depending on the value of $\tilde{\omega}$, the metric function admits different causal configurations, including spacetimes with two distinct horizons (inner and outer), a single degenerate (extremal) horizon, or no horizon at all. The sensitivity of the causal structure of the BRBH to the underlying parameters is consistent with earlier analyses reported in the literature [55]. For each fixed value of M , increasing $\tilde{\omega}$ drives a smooth transition between these causal regimes, highlighting the role of QG corrections in deforming the classical SBH horizon structure. In particular, for $M = 2$, the transition from a two-horizon configuration to a horizonless spacetime occurs at approximately $\tilde{\omega} \simeq 0.8$, while for $M = 5$ this transition shifts to $\tilde{\omega} \simeq 5$. These values mark the boundary between BH and horizonless configurations for the corresponding masses.

III. PHOTON MOTION OF BONANNO–REUTER BH IN PLASMA MEDIUM

The Lagrangian describing a massless test particle (photon) moving in a general static, spherically symmetric spacetime and confined to the equatorial plane ($\theta = \pi/2$) is given by

$$\mathcal{L} = \frac{1}{2} g_{\mu\nu} \dot{x}^\mu \dot{x}^\nu = \frac{1}{2} \left(g_{tt} \dot{t}^2 + g_{rr} \dot{r}^2 + g_{\phi\phi} \dot{\phi}^2 \right). \quad (4)$$

In vacuum, this Lagrangian leads to null geodesic motion for photons. However, in the presence of a plasma medium, photon propagation is no longer governed by null geodesics of the spacetime metric alone. Instead, it is described by an effective Hamiltonian derived from

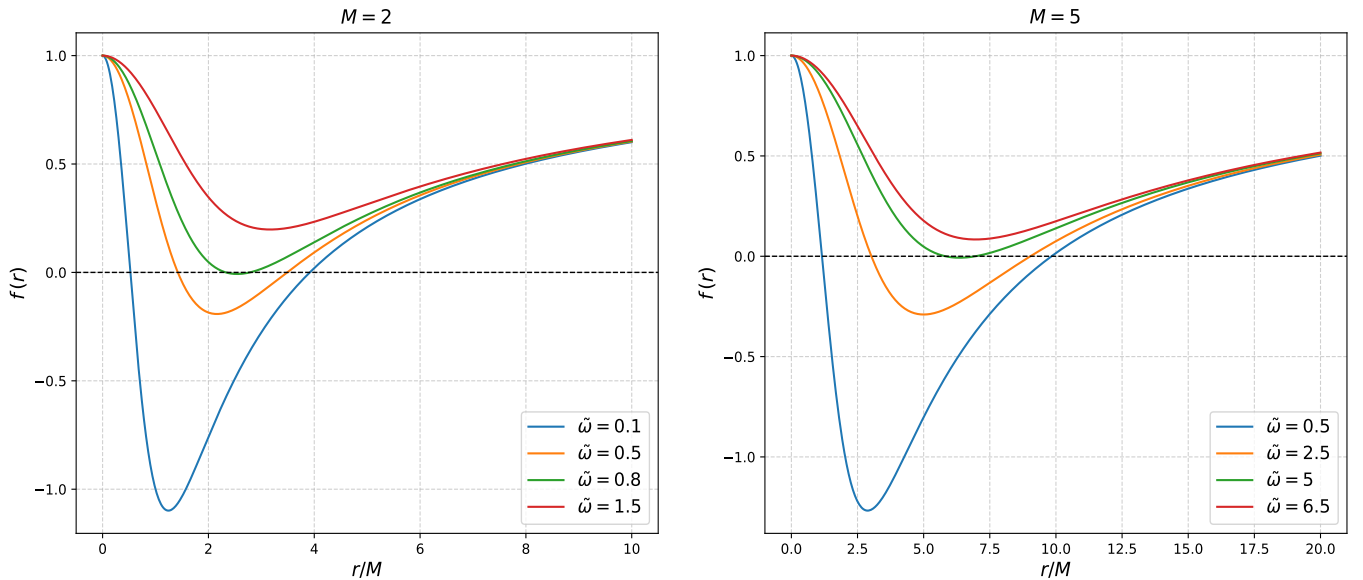


FIG. 1: Variation of the metric function with radial distance for different values of γ , considering (a) $M = 2$ and (b) $M = 3$. We set $G_0 = 1$ and $\gamma = 4.5$.

the dispersion relation in a refractive medium. The corresponding Hamiltonian governing photon propagation in plasma is given by [10],

$$H = \frac{1}{2} (g^{\mu\nu} p_\mu p_\nu + \omega_p^2), \quad (5)$$

where ω_p denotes the plasma frequency, which characterizes the response of the surrounding ionized medium and depends on the local electron number density. For a cold, non-magnetized plasma, it is defined as

$$\omega_p^2(r) = \frac{4\pi e^2}{m_e} N(r), \quad (6)$$

with e and m_e being the electron charge and mass, respectively, and $N(r)$ the electron number density. In the homogeneous case, ω_p can be treated as a constant. However, in the present work, we consider a non-homogeneous plasma environment and model the plasma frequency using a radial power-law profile [25],

$$\omega_p^2(r) = \frac{h}{r^\beta}, \quad (7)$$

where h and β are constants with $\beta \geq 0$. The special case $\beta = 0$ corresponds to a homogeneous plasma. Throughout this work, we consider $\beta = 1$. The presence of plasma introduces a frequency-dependent refractive index, given by

$$n^2 = 1 - \left(\frac{\omega_p}{\omega}\right)^2, \quad (8)$$

where ω denotes the photon frequency measured by a static observer at radius r . Owing to gravitational redshift, this frequency is related to the conserved frequency

ω_0 measured at spatial infinity as

$$\omega = \frac{\omega_0}{\sqrt{-g_{00}}}. \quad (9)$$

Thus, using $p_0 = E_0 = \omega_0$, the Hamiltonian can be rewritten as

$$H = \frac{1}{2} (g^{\mu\nu} p_\mu p_\nu + (n^2 - 1) g^{00} p_0^2). \quad (10)$$

Applying Hamilton's equations, $\dot{p}_\mu = -\partial H / \partial x^\mu$, and noting that the plasma frequency depends only on the radial coordinate, $\omega_p = \omega_p(r)$, we identify the conserved quantities as

$$p_0 = -E, \quad p_\phi = L,$$

where E and L denote the conserved energy and angular momentum of the photon, respectively. The canonical equations lead to the equations of motion in the equatorial plane, given by

$$\frac{dt}{d\lambda} = \frac{n^2 E}{f(r)}, \quad (11)$$

$$\frac{d\phi}{d\lambda} = \frac{L}{r^2}, \quad (12)$$

$$\left(\frac{dr}{d\lambda}\right)^2 = n^2 E^2 - \frac{L^2}{r^2} f(r), \quad (13)$$

where λ is an affine parameter along the photon trajectory, and E and L denote the conserved energy and angular momentum of the photon, respectively. Combining the above equations yields the trajectory equation

$$\left(\frac{dr}{d\phi}\right)^2 = r^4 \left[\frac{n^2(r) E^2}{L^2} - \frac{f(r)}{r^2} \right]. \quad (14)$$

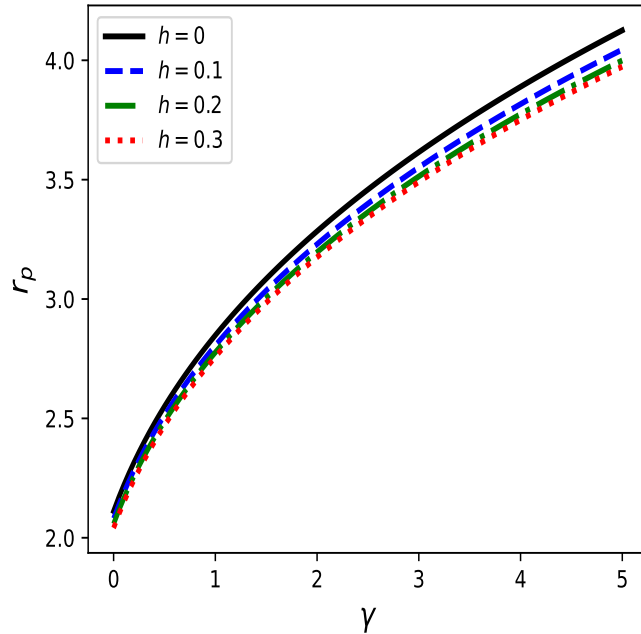


FIG. 2: Variation of radius of photon sphere as a function of γ for different values of h . Parameters are chosen as $M = 5$, $G_0 = 1$, $k_p = 0.5$, and $\tilde{\omega} = 118/(15\pi)$.

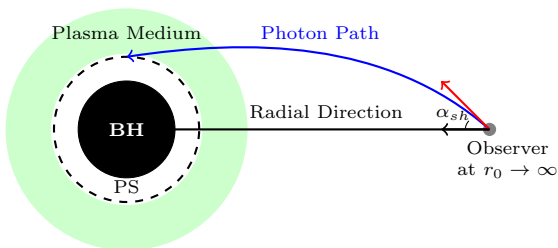


FIG. 3: Schematic representation of photon deflection near a BH surrounded by a plasma medium. α_{sh} is the angular radius of the shadow [33, 56].

The radius of the photon sphere, r_p , in the plasma medium is determined by the existence of unstable circular photon orbits. These satisfy the conditions

$$\dot{r} = 0 \quad \text{and} \quad \frac{d}{dr} (\dot{r}^2) = 0,$$

evaluated at $r = r_p$. Here, the dot denotes differentiation with respect to the affine parameter. Applying these conditions to the radial equation leads to the photon sphere equation

$$\left. \frac{d}{dr} \left(\frac{n^2(r) r^2}{f(r)} \right) \right|_{r=r_p} = 0. \quad (15)$$

Equivalently, this condition can be written in the explicit form

$$\left[2n(r)n'(r) r f(r) + 2n^2(r)f(r) - n^2(r) r f'(r) \right] \Big|_{r=r_p} = 0. \quad (16)$$

The radius of the photon sphere, obtained by numerically solving Eq. 16, is plotted in Fig. 2 as a function of the parameter γ for different values of the plasma exponent h . It is clearly observed that the radius of the photon sphere increases with increasing γ . Furthermore, in the absence of the plasma medium (that is, for negligible plasma density), the radius of the photon sphere attains its maximum value and decreases as the plasma strength parameter h increases.

IV. SHADOW OF THE BLACK HOLE

Astrophysical BHs are often surrounded by ionized matter, forming accretion disks and diffuse plasma clouds [57]. The presence of such plasma environments modifies the propagation of photons through a frequency-dependent refractive index, leading to observable changes in the apparent shadow of the BH. To account for these effects, we consider the propagation of light rays confined to the equatorial plane of the BRBH in the presence of a cold, non-magnetized and inhomogeneous plasma. The schematic figure representing this setup is shown in Fig. 3. Following the standard geometric approach developed by Perlick et al. [22], the angular radius of the shadow as seen by a static observer located at radial coordinate r_0 is given by

$$R_{sh} = \frac{r_p}{\sqrt{f(r_p)}}. \quad (17)$$

Equation (17) allows us to systematically examine

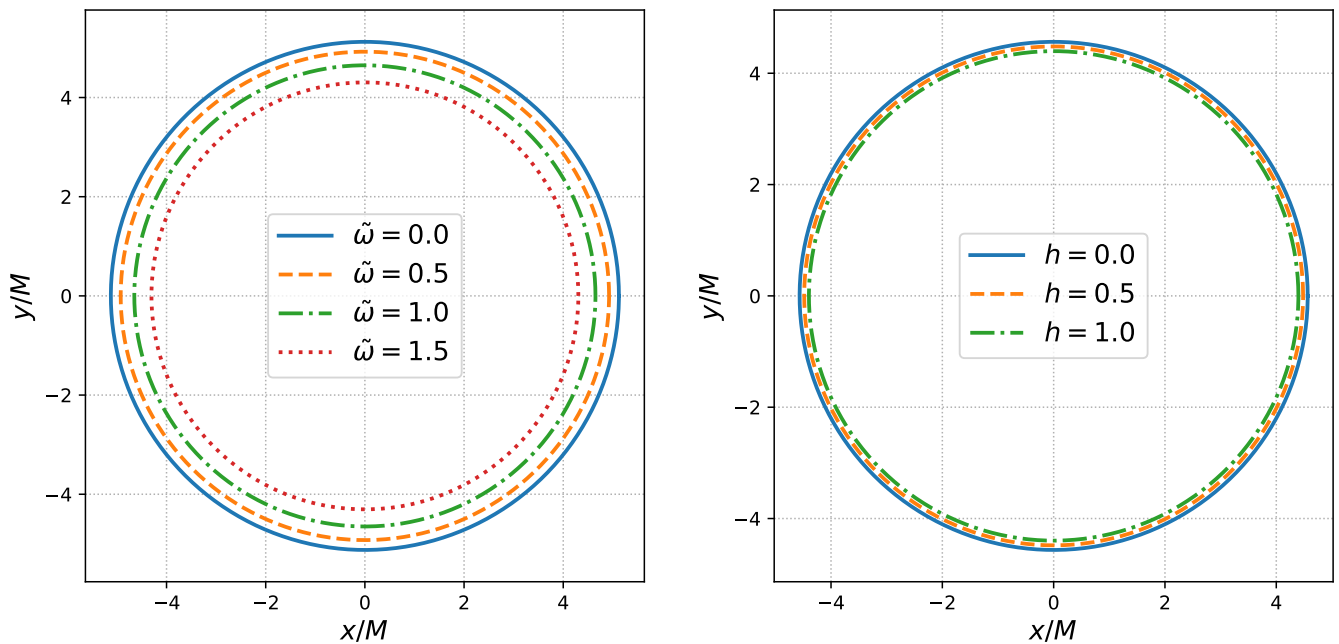


FIG. 4: The angular shadow radius of the BRBH: (a) for different values of the QG correction parameter $\tilde{\omega}$, with the plasma index fixed at $h = 1$ and $\gamma = 4.5$; (b) for different values of the plasma index parameter h , with $\tilde{\omega} = 0.5$ and $\gamma = 4.5$ fixed. Here, x/M and y/M denote the angular celestial coordinates on the observer's sky, normalized by the BH mass M (or equivalently by the shadow radius R_{sh}/M).

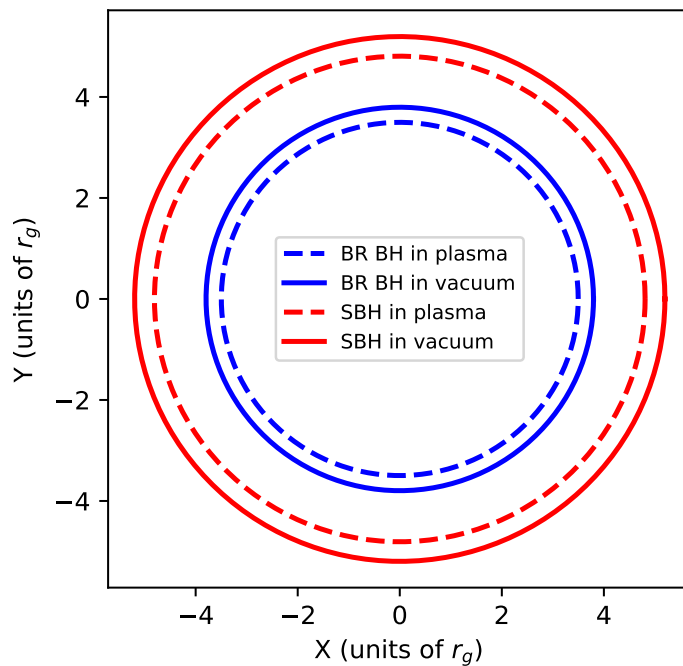


FIG. 5: Comparison of the shadows of the BRBH and SBH, each computed in both vacuum and in the presence of a plasma medium. The parameters are chosen as $M = 1$ for the SBH, $M = 2$ for the BRBH, $G_0 = 1$, $\tilde{\omega} = 0.5$, plasma density falloff index $h = 3$ where applicable, and the parameter $\gamma = 4.5$ fixed for the BRBH. Here, X and Y denote the angular celestial coordinates on the observer's sky, normalized by the BH mass M (or equivalently by the shadow radius R_{sh}/M).

how the shadow of the BRBH varies with the QG correction parameter $\tilde{\omega}$ and the surrounding plasma environment. The corresponding results are shown in Fig. 4. In subfigure (a) of Fig. 4, we fix the plasma parameters and vary $\tilde{\omega}$. The results show that the shadow radius decreases monotonically with increasing $\tilde{\omega}$. This behavior can be physically interpreted as a manifestation of the running of the gravitational coupling constant in the ASG framework: higher values of $\tilde{\omega}$ enhance the effective QG corrections near the horizon, leading to a reduction in the effective gravitational radius and consequently a smaller photon sphere. In other words, the QG corrections act to weaken the spacetime curvature in the near-horizon region, resulting in a reduced apparent shadow size as perceived by a distant observer. Similarly, in subfigure (b) of Fig. 4, we fix $\tilde{\omega}$ and vary the plasma strength. Here, we find that the shadow radius systematically decreases with stronger plasma effects. This behavior arises because a denser plasma increases the local refractive index, which modifies the null geodesics followed by light rays and effectively shrinks the observed angular size of the shadow.

The angular shadow size of the BRBH in plasma reduces to several well-known limiting cases within specific parameter ranges. For instance, setting $h = 0$ reproduces the BRBH in vacuum, setting $\tilde{\omega} = 0$ reproduces the SBH in plasma, and setting both $h = 0$ and $\tilde{\omega} = 0$ reproduces the classical SBH in vacuum. In Fig. 5, we present a qualitative comparison of the four scenarios based on these theoretical results. In the parameter range considered, the shadow sizes decrease successively from the SBH in vacuum to the SBH in plasma, to the BRBH in vacuum, and finally to the BRBH in plasma. This systematic deviation arises from two physical effects. The presence of plasma reduces the shadow size by decreasing the effective speed of light, while quantum corrections in the BRBH reduce the radius of the photon sphere due to the scale dependence of the Newton constant in the RG-improved geometry. Within the considered parameter range, the combined influence of plasma and quantum corrections results in the smallest shadow for the BRBH in plasma. We note that although this behavior is well defined for the chosen parameter values, a broader exploration of plasma densities and quantum correction parameters may lead to partial degeneracies in the observed shadow sizes.

We extend our analysis by constraining the shadow results using observational data from the EHT for Sgr A*. The angular radius of the observed shadow lies within the 1σ band of 4.55–5.22 and the 2σ band of 4.25–5.56 in units of GM/c^2 [58, 59]. We compare our theoretical predictions for the photon sphere radius, considering different plasma profiles and values of the QG correction parameter $\tilde{\omega}$, with these observational limits. The agreement within the 1σ and 2σ confidence intervals serves as a consistency check and helps to assess the physical viability of the proposed model.

Fig. 6 illustrates the normalized shadow radius R_{sh}/M of the BRBH in a plasma environment with QG corrections, compared with the EHT 1σ and 2σ observational bounds for Sgr A*. All theoretical curves lie within the 1σ confidence region, which is itself contained within the 2σ region, indicating that for the considered ranges of the plasma index ($0 \leq h \leq 1.0$) and the QG parameter ($0 \leq \tilde{\omega} \lesssim 0.5$), neither plasma refraction nor quantum corrections lead to shadow sizes inconsistent with current observations. The shadow radius decreases monotonically with increasing plasma index or QG strength, reflecting enhanced light refraction in a denser plasma and modifications of photon trajectories near the BH due to quantum effects. The potential observational degeneracy between plasma and quantum effects is a notable feature, whereby an increase in plasma density can compensate for a smaller quantum correction, and vice versa, leading to similar shadow sizes in observations. However, within the specific limits considered in Fig. 5, a clear and systematic deviation in the shadow sizes is obtained. This comparison is based on a theoretical limiting analysis designed to isolate the deviation from the classical SBH case due to individual plasma and QG parameters. While current EHT observations cannot independently distinguish between plasma-induced and QG-induced modifications, future high-resolution measurements with the next-generation Event Horizon Telescope (ngEHT) are expected to resolve this observational degeneracy and place tighter constraints on the BRBH parameters. The numerical analysis provides upper bounds

TABLE I: Upper bounds on $\tilde{\omega}$ from EHT observations for different plasma indices h .

h	Upper 1σ	Upper 2σ
0.00	1.1791	1.1908
0.10	1.1734	1.5703
0.20	1.1607	1.5149
0.30	1.1639	1.5144
0.40	1.1375	1.5703
0.50	1.1247	1.5325

on the QG parameter $\tilde{\omega}$ for different plasma indices h based on the EHT observational constraints for Sgr A*. The results are summarized in Table I. For $h = 0.0$, the shadow radius allows $\tilde{\omega} \lesssim 1.179$ at the 1σ confidence level and $\tilde{\omega} \lesssim 1.191$ at 2σ . As the plasma index increases, the allowed $\tilde{\omega}$ gradually decreases at 1σ , reaching $\tilde{\omega} \lesssim 1.047$ for $h = 1.0$, while the 2σ bounds vary more irregularly due to wider observational uncertainties, with $\tilde{\omega} \lesssim 3.651$ at $h = 1.0$. This indicates that for moderate plasma densities ($h \lesssim 0.5$), the BRBH remains fully consistent with EHT observations, and even at higher plasma indices, the model predictions stay largely within the 2σ range, highlighting the robustness of the constraints and the degeneracy between plasma effects and QG corrections. We compare our results for a consistency check with the study by Kumar et al. [60], which analyzed the shadow

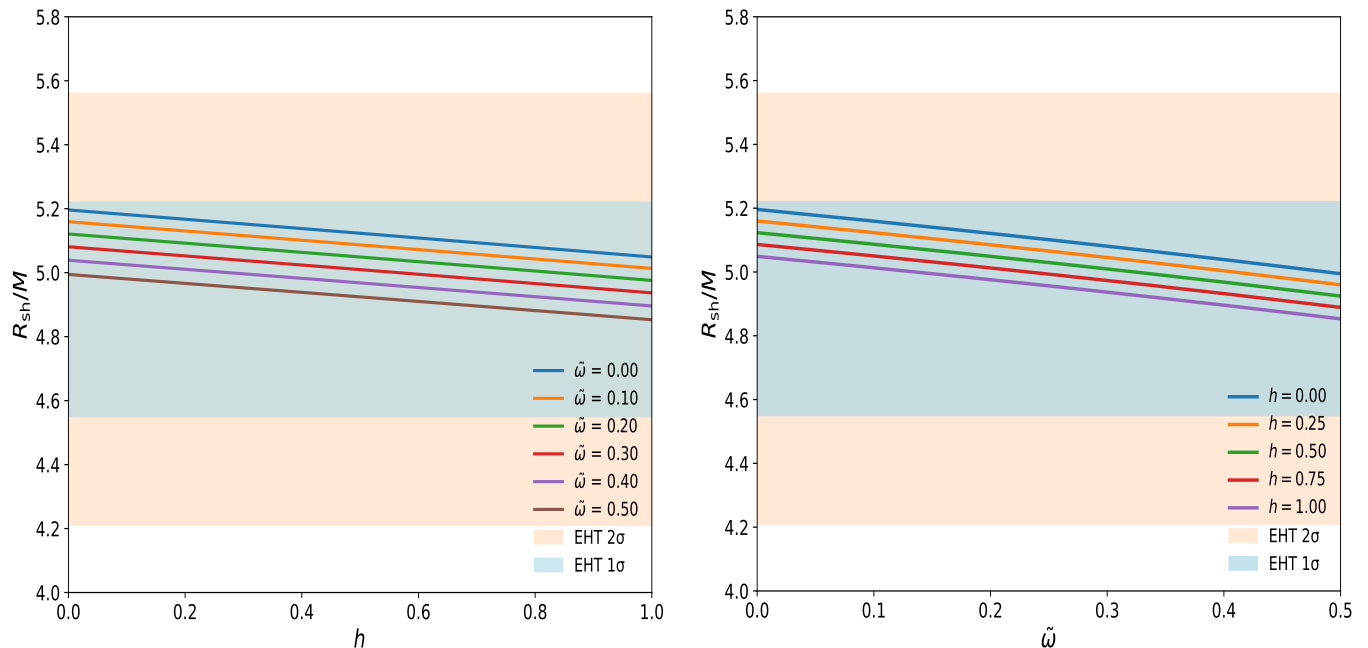


FIG. 6: Shadow radius of the BRBH compared with the EHT observational constraints for Sgr A*, including the 1σ and 2σ confidence regions.

of rotating BHs in ASG. In the limit $\tilde{\omega} = 0$ and in the absence of plasma, our findings qualitatively reproduce the shadow radius and shape trends reported by Kumar et al., confirming consistency with their results. While they observed that the shadow radius decreases and intrinsic distortion increases with larger ζ , we find that increasing the QG parameter $\tilde{\omega}$ similarly reduces the shadow radius. Our work further extends this analysis by including plasma effects, demonstrating that refractive modifications also shrink the apparent shadow size, thereby highlighting the combined impact of QG corrections and environmental effects. Overall, this comparison establishes that our framework is consistent with previous studies while providing additional insights for plasma environments.

V. CONCLUSIONS

In this paper, we investigated the shadow properties of a BRBH in the presence of a non-uniform, magnetized, pressureless cold plasma. The key results are as follows:

- The shadow radius of the BRBH decreases monotonically with increasing QG correction parameter $\tilde{\omega}$, as higher $\tilde{\omega}$ strengthens quantum corrections near the horizon, reducing the effective photon sphere. Similarly, the shadow radius decreases with increasing plasma index h , reflecting enhanced light refraction in a denser plasma. These effects highlight the combined role of spacetime geometry and medium properties in shaping the shadow.

- The angular shadow size of the BRBH in plasma reduces to the corresponding well-known limiting cases, and a qualitative comparison of these scenarios is presented. Within the considered parameter range, the combined effects of plasma and quantum corrections yield the smallest shadow for the BRBH in plasma, clearly demonstrating the deviation from the classical limit.
- The QG correction parameter $\tilde{\omega}$ is constrained using EHT observations of Sgr A* for different plasma indices h . The results indicate that, for moderate plasma densities and quantum corrections, the predicted shadow radius remains within the 1σ confidence region. The upper bounds on $\tilde{\omega}$ decrease slightly as h increases, while the 2σ limits remain more relaxed due to larger observational uncertainties (see Table I).
- The combined influence of plasma effects and QG corrections can lead to an observational degeneracy when constraining the model with EHT data, since an increase in plasma density may compensate for a smaller quantum correction, making it difficult to disentangle the individual effects of these parameters. Future high-resolution observations with the ngEHT are expected to break this degeneracy and place tighter constraints on both the QG parameter $\tilde{\omega}$ and the plasma properties.
- Finally, we compare our results with those of Kumar et al. [60], who analyzed shadows of rotat-

ing BHs in ASG. In the limit $\tilde{\omega} = 0$ and in the absence of plasma, our results qualitatively match their findings.

These results show that both quantum gravitational corrections and plasma effects influence the size of BH shadows. Within the studied parameter range, the shadow sizes follow a predictable pattern, but in a broader parameter space, degeneracies can occur, which may affect observational interpretation. This analysis highlights the need to account for both quantum gravity and astrophysical environments when interpreting horizon-scale BH observations.

Acknowledgments

We thank the referee for the insightful comments, which have significantly improved the presentation and consistency of the manuscript. The author acknowledges the Institute of Mathematical Sciences (IMSc), Chennai for providing excellent research facilities and a conducive environment that supported his work as an Institute Postdoctoral Fellow. The author also gratefully acknowledges the contribution of COST Action CA21136 – “Addressing Observational Tensions in Cosmology with Systematics and Fundamental Physics (CosmoVerse).”

-
- [1] Albert Einstein. The foundation of the general theory of relativity. *Annalen Phys.*, 49(7):769–822, 1916.
- [2] Karl Schwarzschild. On the gravitational field of a mass point according to Einstein’s theory. *Sitzungsber. Preuss. Akad. Wiss. Berlin (Math. Phys.)*, 1916:189–196, 1916.
- [3] Davide Batic, S. Nelson, and M. Nowakowski. Light on curved backgrounds. *Phys. Rev. D*, 91(10):104015, 2015.
- [4] Shubham Kala, Hemwati Nandan, and Prateek Sharma. Deflection of Light Around a Rotating BTZ Black Hole. *Mod. Phys. Lett. A*, 35(39):2050323, 2020.
- [5] Shubham Kala, Hemwati Nandan, Prateek Sharma, and Maye Elmardi. Geodesics and bending of light around a BTZ black hole surrounded by quintessential matter. *Mod. Phys. Lett. A*, 36(31):2150224, 2021.
- [6] Shubham Kala. Propagation of massless particles around a BTZ–ModMax black hole. *International Journal of Geometric Methods in Modern Physics*, 1 2025.
- [7] Subrahmanyan Chandrasekhar. *The mathematical theory of black holes*, volume 69. Oxford university press, 1998.
- [8] Pedro V. P. Cunha, Nelson A. Eiró, Carlos A. R. Herdeiro, and José P. S. Lemos. Lensing and shadow of a black hole surrounded by a heavy accretion disk. *JCAP*, 03:035, 2020.
- [9] Shubham Kala, Saurabh, Hemwati Nandan, and Prateek Sharma. Deflection of light and shadow cast by a dual-charged stringy black hole. *Int. J. Mod. Phys. A*, 35(28):2050177, 2020.
- [10] J. L. Synge. The Escape of Photons from Gravitationally Intense Stars. *Mon. Not. Roy. Astron. Soc.*, 131(3):463–466, 1966.
- [11] J. M. Bardeen. Timelike and null geodesics in the Kerr metric. *Proceedings, Ecole d’Eté de Physique Théorique: Les Astres Occlus : Les Houches, France, August, 1972, 215-240*, pages 215–240, 1973.
- [12] Rohta Takahashi. Black hole shadows of charged spinning black holes. *Publ. Astron. Soc. Jap.*, 57:273, 2005.
- [13] Heino Falcke, Fulvio Melia, and Eric Agol. Viewing the shadow of the black hole at the galactic center. *Astrophys. J. Lett.*, 528:L13, 2000.
- [14] Tim Johannsen and Dimitrios Psaltis. Testing the No-Hair Theorem with Observations in the Electromagnetic Spectrum: II. Black-Hole Images. *Astrophys. J.*, 718:446–454, 2010.
- [15] RA Konoplya. Shadow of a black hole surrounded by dark matter. *Physics Letters B*, 795:1–6, 2019.
- [16] R. A. Konoplya and A. Zhidenko. Shadows of parametrized axially symmetric black holes allowing for separation of variables. *Phys. Rev. D*, 103(10):104033, 2021.
- [17] Kazunori Akiyama et al. First M87 Event Horizon Telescope Results. I. The Shadow of the Supermassive Black Hole. *Astrophys. J. Lett.*, 875:L1, 2019.
- [18] Pedro V. P. Cunha, Carlos A. R. Herdeiro, and Maria J. Rodriguez. Shadows of Exact Binary Black Holes. *Phys. Rev. D*, 98(4):044053, 2018.
- [19] Sunny Vagnozzi et al. Horizon-scale tests of gravity theories and fundamental physics from the Event Horizon Telescope image of Sagittarius A. *Class. Quant. Grav.*, 40(16):165007, 2023.
- [20] Reinhard A Breuer and Jürgen Ehlers. Propagation of high-frequency electromagnetic waves through a magnetized plasma in curved space-time. i. *Proceedings of the Royal Society of London. A. Mathematical and Physical Sciences*, 370(1742):389–406, 1980.
- [21] Russell Kulsrud and Abraham Loeb. Dynamics and gravitational interaction of waves in nonuniform media. *Physical Review D*, 45(2):525, 1992.
- [22] Volker Perlick, Oleg Yu. Tsupko, and Gennady S. Bisnovatyi-Kogan. Influence of a plasma on the shadow of a spherically symmetric black hole. *Phys. Rev. D*, 92(10):104031, 2015.
- [23] Volker Perlick and Oleg Yu. Tsupko. Light propagation in a plasma on Kerr spacetime. II. Plasma imprint on photon orbits. *Phys. Rev. D*, 109(6):064063, 2024.
- [24] Volker Perlick. Characterisation of circular light rays in a plasma. *Class. Quant. Grav.*, 42(17):175013, 2025.
- [25] Adam Rogers. Frequency-dependent effects of gravitational lensing within plasma. *Monthly Notices of the Royal Astronomical Society*, 451(1):17–25, 2015.
- [26] Jan Schee, Zdeněk Stuchlík, Bobomurat Ahmedov, Ahmadjon Abdujabbarov, and Bobir Toshmatov. Gravitational lensing by regular black holes surrounded by plasma. *Int. J. Mod. Phys. D*, 26(5):1741011, 2017.
- [27] Ali Övgün and İzzet Sakallı. Testing generalized Einstein–Cartan–Kibble–Sciama gravity using weak deflection angle and shadow cast. *Class. Quant. Grav.*, 37(22):225003, 2020.
- [28] Allah Ditta, Xia Tiecheng, Farruh Atamurotov, Ibrar Hussain, and G. Mustafa. Particle dynamics, black hole shadow and weak gravitational lensing in the f(Q) theory of gravity. *Commun. Theor. Phys.*, 75(12):125404, 2023.

- [29] Yovqochev Pahlavon, Farruh Atamurotov, Kimet Jusufi, Mubasher Jamil, and Ahmadjon Abdujabbarov. Effect of magnetized plasma on shadow and gravitational lensing of a Reissner–Nordström black hole. *Phys. Dark Univ.*, 45:101543, 2024.
- [30] Fabiano Feleppa, Valerio Bozza, and Oleg Yu. Tsupko. Strong deflection limit analysis of black hole lensing in inhomogeneous plasma. *Phys. Rev. D*, 110(6):064031, 2024.
- [31] Saswati Roy, Shubham Kala, Prasanjit Ghosh, Hemwati Nandan, and Asoke K. Sen. Non-equatorial deflection of light due to Kerr–Newman black hole: a material medium approach. *Eur. Phys. J. C*, 85(8):925, 2025.
- [32] Kirill Kobialko, Dmitri Gal’tsov, and Alexey Molchanov. Gravitational shadow and emission spectrum of thin accretion disks in a plasma medium. *Phys. Rev. D*, 112(4):044039, 2025.
- [33] Gennady S. Bisnovaty-Kogan and Oleg Yu. Tsupko. Gravitational Lensing in Presence of Plasma: Strong Lens Systems, Black Hole Lensing and Shadow. *Universe*, 3(3):57, 2017.
- [34] Farruh Atamurotov and Bobomurat Ahmedov. Optical properties of black hole in the presence of plasma: shadow. *Phys. Rev. D*, 92:084005, 2015.
- [35] Farruh Atamurotov, Mubasher Jamil, and Kimet Jusufi. Quantum effects on the black hole shadow and deflection angle in the presence of plasma. *Chinese Physics C*, 47(3):035106, 2023.
- [36] Ziyodulla Turakhonov, Farruh Atamurotov, Sushant G. Ghosh, and Ahmadjon Abdujabbarov. Probing effects of plasma on shadow and weak gravitational lensing by regular black holes in asymptotically safe gravity. *Phys. Dark Univ.*, 48:101880, 2025.
- [37] İrfan Çimdiker, Durmuş Demir, and Ali Övgün. Black hole shadow in symmergent gravity. *Phys. Dark Univ.*, 34:100900, 2021.
- [38] Riasat Ali, Xia Tiecheng, Rimsha Babar, and Ali Övgün. Exploring light deflection and black hole shadows in rastall theory with plasma effects. *International Journal of Theoretical Physics*, 64(3):75, 2025.
- [39] Riasat Ali, Xia Tiecheng, Rimsha Babar, and Ali Övgün. Exploring Light Deflection and Black Hole Shadows in Rastall Theory with Plasma Effects. *Int. J. Theor. Phys.*, 64(3):75, 2025.
- [40] Abhishek Chowdhuri and Arpan Bhattacharyya. Shadow analysis for rotating black holes in the presence of plasma for an expanding universe. *Phys. Rev. D*, 104(6):064039, 2021.
- [41] Shubham Kala, Hemwati Nandan, and Prateek Sharma. Shadow and weak gravitational lensing of a rotating regular black hole in a non-minimally coupled Einstein–Yang–Mills theory in the presence of plasma. *Eur. Phys. J. Plus*, 137(4):457, 2022.
- [42] Shubham Kala, Hemwati Nandan, Amare Abebe, and Saswati Roy. Gravitational lensing around a dual-charged stringy black hole in plasma background. *Eur. Phys. J. C*, 84(10):1089, 2024.
- [43] Shubham Kala and Jaswinder Singh. Gravitational lensing and shadow around a non-minimally coupled Horndeski black hole in plasma medium. *Eur. Phys. J. C*, 85(9):1047, 2025.
- [44] Alfio Bonanno and Martin Reuter. Renormalization group improved black hole space-times. *Phys. Rev. D*, 62:043008, 2000.
- [45] Alessia Platania. Black holes in asymptotically safe gravity. In *Handbook of quantum gravity*, pages 1–65. Springer, 2023.
- [46] Nisha Godani and Shubham Kala. A new class of generalized Ellis–Bronnikov wormhole in asymptotically safe gravity. *Int. J. Mod. Phys. D*, 32(10):2350067, 2023.
- [47] M. Reuter and E. Tuiran. Quantum Gravity Effects in the Kerr Spacetime. *Phys. Rev. D*, 83:044041, 2011.
- [48] Daniel Becker and Martin Reuter. Running boundary actions, Asymptotic Safety, and black hole thermodynamics. *JHEP*, 07:172, 2012.
- [49] Thomas Burschil and Benjamin Koch. Renormalization group improved black hole space-time in large extra dimensions. *Zh. Eksp. Teor. Fiz.*, 92:219–225, 2010.
- [50] Yun-Xian Chen, Ping-Hui Mou, and Guo-Ping Li. The Observational Shadow Features of a Renormalization Group Improved Black Hole Considering Spherical Accretions. *Symmetry*, 14(10):1959, 2022.
- [51] Luis A. Sánchez. Shadow of a renormalization group improved rotating black hole. *Eur. Phys. J. C*, 84(10):1056, 2024.
- [52] Mrinnoy M. Gohain, Hari Prasad Saikia, Chayanika Chetia, Pratiba Gohain, and Kalyan Bhuyan. Shadows of Renormalisation Group Improved Black Holes Surrounded by Plasma. *J. Phys. Conf. Ser.*, 2957(1):012019, 2025.
- [53] R. A. Konoplya, Z. Stuchlik, A. Zhidenko, and A. F. Zinhailo. Quasinormal modes of renormalization group improved Dymnikova regular black holes. *Phys. Rev. D*, 107(10):104050, 2023.
- [54] S. V. Bolokhov and Milena Skvortsova. Gravitational Quasinormal Modes and Grey-Body Factors of Bonanno-Reuter Regular Black Holes. *Theor. Phys.*, 1:3, 2025.
- [55] Raúl Carballo-Rubio et al. Towards a non-singular paradigm of black hole physics. *JCAP*, 05:003, 2025.
- [56] Saswati Roy, Shubham Kala, Atanu Singha, Hemwati Nandan, and Asoke K. Sen. Deflection of light due to Kerr Sen black hole in heterotic string theory using material medium approach. *Eur. Phys. J. C*, 85(7):772, 2025.
- [57] Dmitri A. Uzdensky and Shane Rightley. Plasma Physics of Extreme Astrophysical Environments. *Rept. Prog. Phys.*, 77:036902, 2014.
- [58] Kazunori Akiyama et al. First Sagittarius A* Event Horizon Telescope Results. I. The Shadow of the Supermassive Black Hole in the Center of the Milky Way. *Astrophys. J. Lett.*, 930(2):L12, 2022.
- [59] Shubham Kala, Hemwati Nandan, Kush Maithani, Saswati Roy, and Amare Abebe. Null geodesics, thermodynamics, weak gravitational lensing, and black hole shadow characteristics of a Frolov regular black hole with constraints from EHT observations. *Eur. Phys. J. Plus*, 140(10):991, 2025.
- [60] Rahul Kumar, Balendra Pratap Singh, and Sushant G. Ghosh. Shadow and deflection angle of rotating black hole in asymptotically safe gravity. *Annals Phys.*, 420:168252, 2020.